ACS Catalysis

Research Article

pubs.acs.org/acscatalysis

Rapid and Complete Removal of Nonylphenol by Gold Nanoparticle/Rutile Titanium(IV) Oxide Plasmon Photocatalyst

Shin-ichi Naya,[†] Tomoyuki Nikawa,[‡] Keisuke Kimura,[‡] and Hiroaki Tada*[,†,‡]

[†]Environmental Research Laboratory and [‡]Department of Applied Chemistry, School of Science and Engineering, Kinki University, 3-4-1, Kowakae, Higashi-Osaka, Osaka 577-8502, Japan

ABSTRACT: Nonylphenol is a harmful endocrine disruptor, and the concentration in ambient water should be restricted below 0.1 μM. We show that visible-light irradiation of gold nanoparticle (NP)-loaded rutile TiO_2 (Au/rutile TiO_2) plasmon photocatalyst leads to rapid and complete removal of nonylphenol from its dilute aqueous solution with the degradation. Au/rutile TiO_2 exhibits much higher visible-light activity than Au/anatase TiO_2 and $BiVO_4$. Based on the results of the adsorption and Fourier-transformed infrared spectroscopic measurements, we present a unique reaction scheme consisting of a series of events, the fast oxidative adsorption and concentration of nonylphenol on the Au NP surface, the successive efficient oxidation induced by the localized surface plasmon resonance excitation-driven interfacial electron transfer from Au NP to rutile TiO_2, and the regeneration of the adsorption sites by the surface transport of the intermediates from Au to TiO_2.

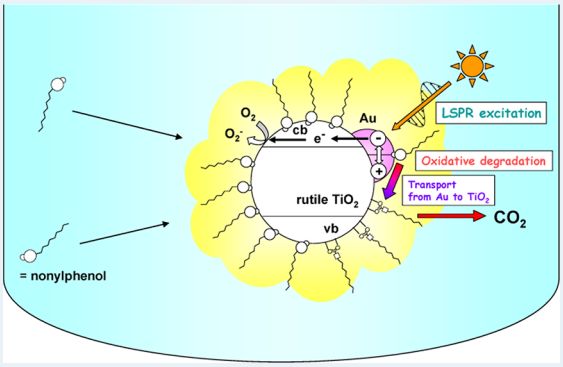

KEYWORDS: *plasmon photocatalyst, Au nanoparticle, rutile TiO_2, nonylphenol, water purification*

INTRODUCTION

Phenol derivatives are useful starting materials for many industrial chemical products, e.g., *p*-cresol for an antiseptic substance, 2-naphthol for azo dyes, and bisphenol A for polycarbonate. Among them, nonylphenol is a very serious endocrine disruptor, and the concentration in ambient water should be restricted < 0.1 μM so as not to exert a baneful effect on living life (Table 1).[1−3] While nonylphenols are widely used as emulsifiers, detergents, surface modifiers, and flotation and dispersing agents, ion−ionic surfactants in wastewater can undergo biodegradation to yield them.[4] Thus, the development of an energy-saving process for completely removing phenol derivatives, particularly nonylphenol, from the wastewater is of great importance for environmental conservation. Since the pioneering work by Pelizzetti and co-workers,[5] the degradation of nonylphenol and its derivatives using TiO_2-based UV-light photocatalysts has been studied.[6−12] In view of the energy and environmental issue, effective utilization of sunlight as an energy source is desirable. Although several visible-light photocatalysts such as $BiVO_4$ and Ag-loaded $BiVO_4$ were used for the nonylphenol degradation,[13,14] these reactions require highly alkaline conditions. On the other hand, gold nanoparticles (NPs) possess the strong visible light absorption due to localized surface plasmon resonance (LSPR).[15,16] As a new type of visible-light photocatalyst, the LSPR-driven photocatalyst called a "plasmon photocatalyst" has recently attracted much attention.[17−25] Gold NP-loaded TiO_2 (Au/TiO_2) plasmon photocatalyst has mainly been applied for organic synthesis, i.e., the selective oxidations of alcohols to carbonyl compounds,[26−29] thiols to disulfides,[30] benzene to phenols,[31,32] and amine to imines.[33] The difference in the molecular structures between *p*-cresol and 4-nonylphenol is only the length of the alkyl chain (Table 1). The strong

Table 1. Molecular Structure and Median Lethal Concentration [LC_{50} (96 h)] for Rainbow Trout (Oncorhynchus Mykiss) of Phenol Derivatives

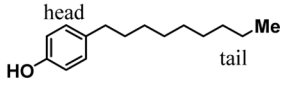 4-nonylphenol	0.43 μM		
 phenol	112 μM	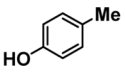 *p*-cresol	73 μM
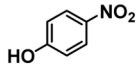 4-nitrophenol	8.6 μM	 catecol	81 μM
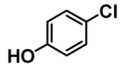 4-chlorophenol	15 μM	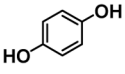 hydroquinone	5.8 μM

Received: December 24, 2012
Published: March 19, 2013

   dx.doi.org/10.1021/cs400169u | *ACS Catal.* 2013, 3, 903−907

endocrine disruption of nonylphenols results from coupling to the estrogen receptor, for which the phenol moiety and the long alkyl chain should be responsible. The decomposition of either of them would be sufficient for getting rid of or reducing its high risk.[34,35]

Here we show that the Au/rutile TiO_2 (Au/rutile) plasmon photocatalyst oxidizes nonylphenol to rapidly reduce the concentration to a permitted level (<0.1 μM) by visible-light irradiation. Further, the origin is studied by comparing the adsorption property and the photocatalytic activities of Au/rutile and Au/anatase for nonylphenol and *p*-cresol.

EXPERIMENTAL SECTION

Photocatalyst Synthesis. Au particles were loaded on anatase TiO_2 particles with a specific surface area of 8.1 m^2 g^{-1} (A-100, Ishihara Sangyo, mean particle size = 150 nm) and on rutile TiO_2 particles with a specific surface area of 12.5 m^2 g^{-1} (TAYCA, mean particle size = 100 nm) by the deposition–precipitation (DP) method using $HAuCl_4$ as a starting material.[36,37] The mean diameters of the Au NPs were determined by transmission electron microscopy at an applied voltage of 300 kV (JEM-3010, JEOL). The loading amount of Au was quantified by inductively coupled plasma spectroscopy (ICPS-7500, Shimadzu).

Au/TiO_2-Photocatalyzed Degradation of Nonylphenol. After the suspension of Au/TiO_2 (100 mg) in a solution of nonylphenol (50 μM) in H_2O:acetonitrile (9:1, 0.1 L) had been stirred at 298 K in the dark for 15 min, irradiation was started using a 300 W Xe lamp (HX-500, Wacom) with a cut off filter Y-45 (AGC TECHNO GLASS) in a double jacket type reaction cell (45 mm in diameter and 80 mm in length). The light intensity integrated from 420 to 485 nm ($I_{420-485}$) through a Y-45 optical filter was adjusted to 6.0 mW cm^{-2}. The concentration of nonylphenol was determined by high-performance liquid chromatography (LC-6 AD, SPD-6 A, C-R8A (Shimadzu)) [measurement conditions: column = Shim-pack CLC-ODS (4.6 mm × 150 mm) (Shimadzu); mobile phase acetonitrile; flow rate = 1.0 mL min^{-1}; λ = 277 nm].

Adsorption Measurement. Adsorption isotherms were obtained by exposing Au/rutile TO_2 or rutile TO_2 (10 mg) to solutions (10% or 100% acetonitrile) with different concentrations of nonylphenol solution (10 mL) at 298 K for 4 h in the dark. The concentration of nonylphenol in the solution was quantified by high-performance liquid chromatography.

RESULTS AND DISCUSSION

Au/TiO_2 was prepared by the deposition–precipitation method using NaOH as a neutralizer.[36,37] Figure 1A shows transmission electron micrographs (TEM) of Au/rutile. Uniform Au NPs are highly dispersed on the surface of TiO_2 (mean particle size = 100 nm). The mean particle size (d) of Au NPs was 2.1 nm. Figure 1B shows UV–visible absorption spectra of rutile TiO_2 without and with Au NPs. Loading Au NPs on TiO_2 causes strong and broad absorption due to the Au NP LSPR in the visible region, whereas TiO_2 has only interband transition below ~ 400 nm.

Visible light-induced degradation of nonylphenol was carried out as follows. Aqueous solution of 50 μM nonylphenol containing 10% MeCN, which was added to completely dissolve nonylphenol in water, was prepared. Au/TiO_2 (0.1 g) was added to the solution (0.1 L). After the suspension was stirred in the dark for 0.25 h, visible light (Xe lamp, λ > 430 nm) was irradiated under aerobic conditions. Figure 2 shows the change in the nonylphenol concentration in the presence of various photocatalysts. In the Au/rutile and Au/anatase systems, a large amount of nonylphenol is adsorbed in the dark. However, the concentration is almost invariant without light irradiation. It is worth noting that, in the Au/rutile system, visible-light irradiation gives rise to complete removal of nonylphenol within 2 h of irradiation time (t_p), and no byproduct was observed in the solution. After the reaction, the Au/rutile particles were sufficiently washed with MeCN, and no nonylphenol was detected from the solution. At t_p = 18 h, CO_2 generation was observed witha 3.7 equivalent amount to that of the initial nonylphenol. This fast degradation of nonylphenol needed the visible light irradiation, the aerobic conditions, and Au NP loading. Further, the effect of Au loading amount was investigated. Figure 3A shows time courses for the nonylphenol degradation in the presence of Au/rutile with various Au loading amounts. As the Au loading amount increases, the catalytic activity slightly increases. The complete removal of nonylphenol is achieved at t_p = 1.5 h by the Au(1.68 mass %)/rutile. Figure 3B shows the plots of initial rate (v_0) as a function of Au loading amount. The v_0 value reaches almost constant above 0.56 Au mass %.

To investigate the reaction mechanism, the photonic efficiency (ϕ, molecules decomposed/incident photons) for the nonylphenol degradation was measured by using various optical filters.[38] Figure 4 compares the action spectrum of the ϕ value and the absorption spectrum for Au/rutile. The good resemblance of the profiles clearly indicates that the excitation of the Au NP-LSPR is the driving force for the nonylphenol degradation. The degradation rate for Au/rutile far exceeds those for Au/anatase and $BiVO_4$. Recently, we have reported that Au/rutile shows much higher visible-light activity than Au/

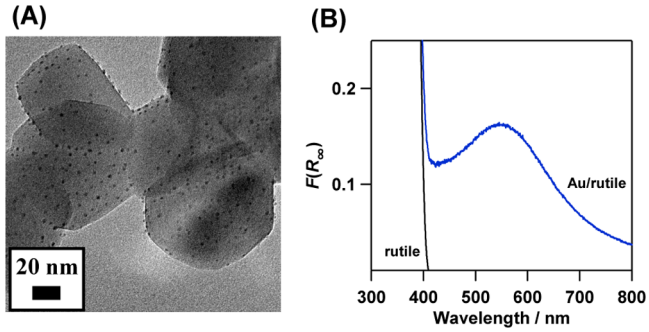

Figure 1. (A) TEM of Au/rutile. (B) UV–vis absorption spectra of rutile and Au/rutile: $F(R_\infty)$ denotes the Kubelka–Munk function corresponding to the absorption intensity.

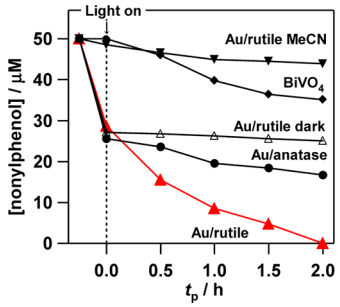

Figure 2. Time courses for nonylphenol degradation.

dx.doi.org/10.1021/cs400169u | ACS Catal. 2013, 3, 903–907

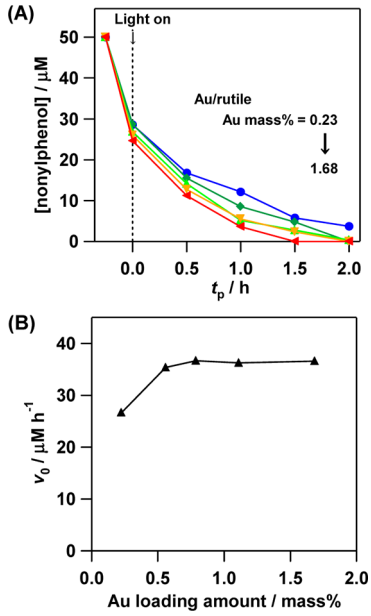

Figure 3. (A) Time courses for nonylphenol decomposition by Au/rutile with varying Au loading amount. (B) Plots of initial rate (v_0) as a function of Au loading amount.

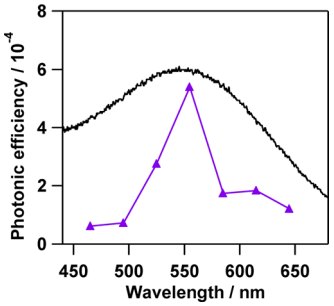

Figure 4. Action spectrum of photonic efficiency (violet) and UV−vis absorption spectrum of Au/rutile (black).

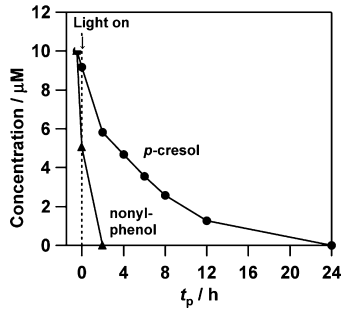

Figure 5. Time courses for Au/rutile-photocatalzyed decompositions of *p*-cresol and nonylphenol.

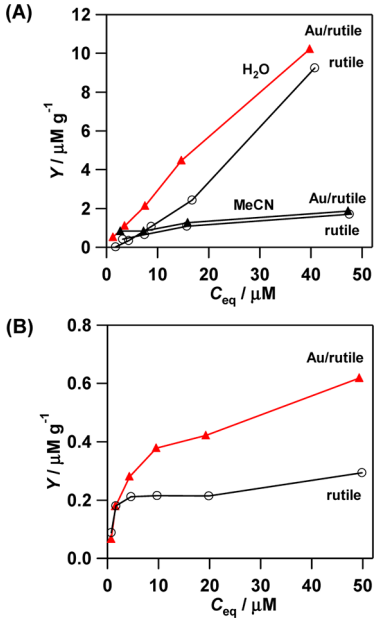

Figure 6. Adsorption isotherms of nonylphenol (A) and *p*-cresol (B) on rutile TiO_2 (empty circle) and Au/rutile TiO_2 (triangle) at 298 K.

anatase for the oxidations of alcohols[28] and amines.[33] Further this remarkable supporting effect was ascribable to the efficient LSPR-driven electron transfer from Au to rutile TiO_2. The same explanation would be valid also for the present system. On the other hand, the conduction band (CB) minimum of $BiVO_4$ is too low to efficiently reduce O_2, and the adsorptivity of $BiVO_4$ for nonylphenol is poor.[13,39] These features explain its low activity. Also, replacing the solvent by 100% MeCN drastically decreases the adsorption in the dark, retarding the rate of reaction. This finding suggests that the adsorption of nonylphenol on the photocatalysts greatly affects their activity.

The visible-light activity of Au/rutile for the degradations of nonylphenol and *p*-cresol was studied. Figure 5 compares time courses for the Au/rutile-photocatalzyed degradations of nonylphenol and *p*-cresol. It takes ∼24 h for the complete removal of *p*-cresol, whereas the removal of nonylphenol is accomplished within 2 h. Evidently, the rapid nonylphenol degradation originates from its long alkyl chain.

To clarify the reason, the adsorption property for nonylphenol was examined in an aqueous MeCN solution (water: MeCN = 9: 1 v/v) and 100% MeCN. Figure 6A shows the adsorption isotherms for nonylphenol on rutile and Au/rutile at 298 K: Y and C_{eq} denote the equilibrium adsorption amount per unit mass of the solid and the equilibrium concentration of nonylphenol, respectively. In the aqueous solution, rutile has good adsorptivity for nonylphenol, and loading a small amount of Au NP further increases the adsorption amount by 0.5−2 μmol g^{-1}. At Au loading amount = 0.56 mass % and d = 2.1 nm, the surface area of Au NPs on TiO_2 occupies only ∼5% of the total surface area. This fact means that the nonylphenol is adsorbed on the surface of Au NP in preference to rutile. Nonylphenol could strongly adsorbed on the surface of Au NPs due to the strong interaction between Au and phenol with the extended π-system. In 100% MeCN, the adsorption amounts on rutile and Au/rutile drastically decrease. Figure 6B shows that the adsorption amounts of *p*-cresol on rutile and Au/rutile from the aqueous solution were much smaller than those of nonylphenol. These results strongly suggest that the striking adsorptivity of Au/rutile for nonylphenol stems from both the Au NP−phenol head interaction and the intermolecular interaction through the long tails.

To study the adsorption states of nonylphenol on Au/rutile before and after visible-light irradiation at a molecular level, UV−visible absorption spectra and diffuse reflectace Fourier-transformed infrared (DRIFT) spectra were measured. Figure 7 shows the UV−visible absorption spectra. The nonylphenol adsorption on Au/rutile causes a slight red-shift in the LSPR peak of Au NPs probably due to the decrease in their electron

dx.doi.org/10.1021/cs400169u | *ACS Catal.* 2013, 3, 903−907

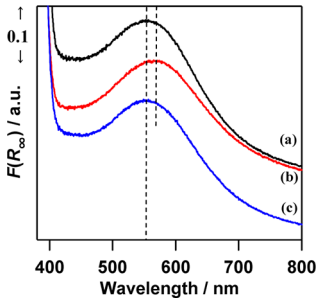

Figure 7. UV–vis absorption spectra of pristine Au/rutile (a, black), nonylphenol-adsorbed Au/rutile before (b, red) and after (c, blue) visible-light irradiation.

density with the adsorption through the back-donation from the phenol moiety of nonylphenol to Au.[40] The peak position is reverted by visible-light irradiation, which indicates clean Au surfaces are recovered. No absorption of nonylphenol and photodegraded intermediates adsorbed on the catalysts was observed due to the intense absorption of rutile in the UV range.

Figure 8 shows DRIFT spectra of Au/rutile (a, black) and nonylphenol-adsorbed Au/rutile before (b, red) and after (c, blue) visible-light irradiation. In spectrum (b), the peaks of the alkyl group and phenol moiety of nonylphenol are observed at 2965 ($\nu_{as}(CH_3)$), 2950 ($\nu_{as}(CH_2)$), 2878 ($\nu_s(CH_3$, $CH_2)$), 1505 (ν(C=C)), 1456 ($\delta_s(CH_2)$), 1379 ($\delta_s(CH_3)$), and 1258 (ν(C–O)) cm^{-1} in addition to the stretching vibration of the surface Ti–OH group at ~3700 cm^{-1}. Unexpectedly, visible-light irradiation intensifies the signals of the alkyl groups in spectrum (c). At the same time, new peaks appear at 1588 and 1418 cm^{-1} assignable to the antisymmetric ($\nu_{as}(COO^-)$) and symmetric ($\nu_s(COO^-)$) stretching vibrations of the carboxylate groups.[41] In the $BiVO_4$-photocatalyzed oxidation of nonylphenol, the cleavage of the phenol ring was shown to generate the carboxylic acid derivatives.[13] The difference of the peaks between $\nu_{as}(COO^-)$ and $\nu_s(COO^-)$ ($\Delta\nu$ = 170 cm^{-1}) suggests that the carboxylate is adsorbed on the TiO_2 surface with a bridging structure as proposed for the dye adsorption on TiO_2 in the dye-sensitized solar cells.[42,43]

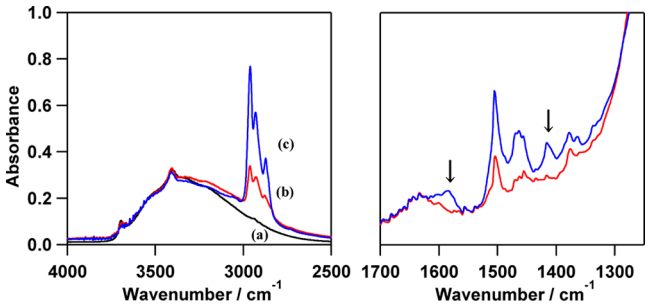

Figure 8. DRIFT spectra of pristine Au/rutile (a, black) and nonylphenol-adsorbed Au/rutile before (b, red) and after (c, blue) visible-light irradiation.

On the basis of these results, we present a reaction scheme for the present rapid and complete removal of nonylphenol by Au/rutile plasmon photocatalyst (Scheme 1). A large amount of nonylphenol is adsorbed and concentrated near the surface of Au NPs because of the strong Au–head interaction and the intermolecular interaction between the tails. Visible-light irradiation induces the efficient electron transfer from Au to rutile, and Au NPs with lowered Fermi energy oxidizes to cleave the benzene ring of nonylphenol adsorbed on their surface. The resulting intermediates with carboxylate group migrate from Au to TiO_2 due to the chemisorption on the TiO_2 surface. The intermediates undergo further oxidation to yield CO_2 at the periphery between Au NP and TiO_2. Also, the recovered clean Au surface acts again as the adsorption and the visible-light-driven oxidation sites. Recently, it has been reported that Au/TiO_2 plasmon photocatalyst possesses the oxidation ability to completely decompose phenol to CO_2 via carboxylic acids.[34] Consequently, the removal of nonylphenol with its degradation continues to be accomplished even under such a low concentration.

Scheme 1. Proposed Mechanism of Nonylphenol Degradation by Au/Rutile TiO_2 Plasmon Photocatalyst

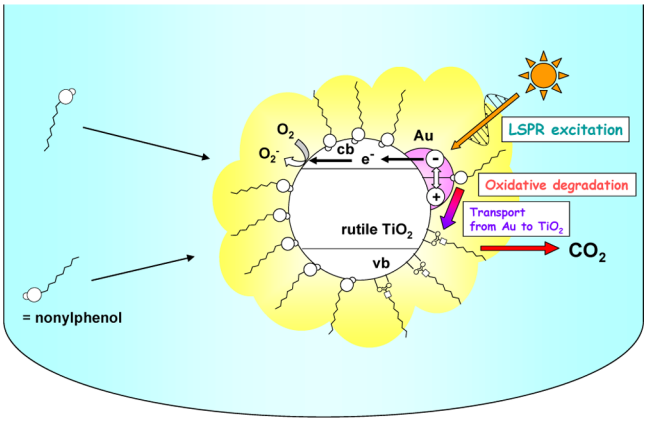

CONCLUSIONS

We have shown that the Au/rutile TiO_2 plasmon photocatalyst gives rise to rapid and complete removal of nonylphenol from its very dilute solution. This study would present an energy-saving technique for the efficient removal of nonylphenol and the analogues, harmful endocrine disruptors.

AUTHOR INFORMATION

Corresponding Author

*E-mail: h-tada@apch.kindai.ac.jp.

Notes

The authors declare no competing financial interest.

ACKNOWLEDGMENTS

Ishihara Sagyo Co. and TAYCA Co. kindly gifted us with A-100 and rutile TiO_2, respectively. This work was partially supported by a Grant-in-Aid for Scientific Research (C) No. 24550239, by Nippon Sheet Glass Foundation for Materials Science and Engineering, and by Sumitomo Foundation.

REFERENCES

(1) United States Environmental Protection Agency (U.S. EPA). Criterion Maximum Concentration. *Clean Water Act of 1972*, Section 304(a), Aquatic life criteria.
(2) U.S. EPA. AQUIRE in *ECOTOX* database.
(3) Eco-toxicity tests of chemicals conducted by Ministry of the Environment in JAPAN based on OECD test guideline, 2009.
(4) Giger, W.; Brunner, P. H.; Schaffner, C. *Science* **1984**, *225*, 623.
(5) Pelizzetti, E.; Minero, C.; Maurino, V.; Sclafani, A.; Hidaka, H.; Serpone, N. *Environ. Sci. Technol.* **1989**, *23*, 1380.

(6) Hoffmann, M. R.; Martin, S. T.; Choi, W.; Bahnemann, D. W. *Chem. Rev.* **1995**, *95*, 69.
(7) Ooka, C.; Yoshida, H.; Horio, M.; Suzuki, K.; Hattori, T. *Appl. Catal. B: Environmental* **2003**, *41*, 313.
(8) Inumaru, K.; Murashima, M.; Kasahara, T.; Yamanaka, S. *Appl. Catal. B: Environmental* **2004**, *52*, 275.
(9) Inumaru, K.; Kasahara, T.; Yasui, M.; Yamanaka, S. *Chem. Commun.* **2005**, 2131.
(10) Ide, Y.; Koike, Y.; Ogawa, M. *J. Colloid Interface Sci.* **2011**, *358*, 245.
(11) Anandan, S.; Ashokkumar, M. *Ultrason. Sonochem.* **2009**, *16*, 316.
(12) Park, H.; Park, Y.; Kim, W.; Choi, W. *J. Photochem. Photobiol., Part C* **2012**, DOI: 10.1016/j.jphotochemrev.2012.10.001.
(13) Kohtani, S.; Koshiko, M.; Kudo, A.; Tokumura, K.; Ishigaki, Y.; Toriba, A.; Hayakawa, K.; Nakagaki, R. *Appl. Catal., B* **2003**, *46*, 573.
(14) Kohtani, S.; Hiro, J.; Yamamoto, N.; Kudo, A.; Tokumura, K.; Nakagaki, R. *Catal. Commun.* **2005**, *6*, 185.
(15) Kreibig, U.; Vollmer, M. *Optical Properties of Metal Clusters*; Springer: Berlin, 1995.
(16) Bohren, C. F.; Huffman, D. R. *Absorption and Scattering of Light by Small Particles*; Wiley: New York, 1983.
(17) Kubacka, A.; Fernandez-Garcia, M.; Colon, G. *Chem. Rev.* **2012**, *112*, 1555.
(18) Wen, B.; Ma, J.-H.; Chen, C.-C.; Ma, W.-H.; Zhu, H.-Y.; Chao, J.-C. *Sci. China, Chem.* **2011**, *54*, 887.
(19) Silva, C. G.; Juárez, R.; Marino, T.; Molinari, R.; García, H. *J. Am. Chem. Soc.* **2011**, *133*, 595.
(20) Yuzawa, H.; Yoshida, T.; Yoshida, H. *Appl. Catal., B* **2012**, *115*−*116*, 294.
(21) Alvaro, M.; Cojocaru, B.; Ismail, A. A.; Petrea, N.; Ferrer, B.; Harraz, F. A.; Parvulescu, V. I.; García, H. *Appl. Catal., B* **2010**, *99*, 191.
(22) Primo, A.; Marino, T.; Corma, A.; Molinari, R.; García, H. *J. Am. Chem. Soc.* **2011**, *133*, 6930.
(23) Liu, Z.; Hou, W.; Pavaskar, P.; Aykol, M.; Cronin, S. B. *Nano Lett.* **2011**, *11*, 1111.
(24) Wand, P.; Huang, B.; Qin, X.; Zhang, X.; Dai, Y.; Wei, J.; Whangbo, M.-H. *Angew. Chem., Int. Ed.* **2008**, *48*, 7931.
(25) Wang, P.; Huang, B.; Dai, Y.; Whangbo, M.-H. *Phys. Chem. Chem. Phys.* **2012**, *14*, 9813.
(26) Kowalska, E.; Abe, R.; Ohtani, B. *Chem. Commun.* **2009**, 241.
(27) Naya, S.; Inoue, A.; Tada, H. *J. Am. Chem. Soc.* **2010**, *132*, 6292.
(28) Kimura, K.; Naya, S.-i.; Jin-nouchi, Y.; Tada, H. *J. Phys. Chem. C* **2012**, *116*, 7111.
(29) Tsukamoto, D.; Shiraishi, Y.; Sugano, Y.; Ichikawa, S.; Tanaka, S.; Hirai, T. *J. Am. Chem. Soc.* **2012**, *134*, 6309.
(30) Naya, S.; Teranishi, M.; Isobe, T.; Tada, H. *Chem. Commun.* **2010**, *46*, 815.
(31) Ide, Y.; Matsuoka, M.; Ogawa, M. *J. Am. Chem. Soc.* **2010**, *132*, 16762.
(32) Zheng, Z.; Huang, B.; Qin, X.; Zhang, X.; Dai, Y.; Wei, J.; Whangbo, M.-H. *J. Mater. Chem.* **2011**, *21*, 9079.
(33) Naya, S.; Kimura, K.; Tada, H. *ACS Catal.* **2013**, *3*, 10.
(34) Zielińska-Jurek, A.; Kowalska, E.; Sobczak, J. W.; Lisowski, W.; Ohotani, B.; Zaleska, A. *Appl. Catal., B* **2011**, *101*, 504.
(35) Kochuveedu, S. T.; Kim, D.-P.; Kim, D. H. *J. Phys. Chem. C* **2012**, *116*, 2500.
(36) Tsubota, S.; Haruta, M.; Kobayashi, T.; Ueda, A.; Nakahara, Y. *Preparation of Catalysis V*; Elsevier: Amsterdam, 1991.
(37) Tada, H.; Kiyonaga, T.; Naya, S.-i. *Metal Oxide-Supported Gold Nanoparticles*; Lambert Academic Publishing: 2012.
(38) Naya, S.; Inoue, A.; Tada, H. *ChemPhysChem* **2011**, *12*, 2719.
(39) Long, M.; Cai, W.; Kisch, H. *J. Phys. Chem. C* **2008**, *112*, 548.
(40) Mulvaney, P.; Giersig, M.; Henglein, A. *J. Phys. Chem.* **1992**, *96*, 10419.
(41) Finne, K. S.; Bartlett, J. R.; Woolfrey, J. L. *Langmuir* **1998**, *14*, 2744.
(42) Nakamoto, K. *Infrared and Raman Spectra of Inorganic and Coordination Compounds, Part B: Applications in Coordination, Organometallic, and Bioinorganic chemistry*, 6th ed.; Wiley-Interscience: New York, 2009.
(43) Lee, K. E.; Gomez, M. A.; Elouatik, S.; Demopoulos, G. P. *Langmuir* **2010**, *26*, 9575.